Influence of heat treatment on LiNbO₃ thin films prepared on Si(111) by the polymeric precursor method

$LiNbO_3$ → Influence of heat treatment on $LiNbO_3$ thin films prepared on Si(111) by the polymeric precursor method

V. Bouquet, E. Longo, and E.R. Leite[a]

*Departamento de Química, LIEC, Universidade Federal de São Carlos, P.O. Box 676,
13565-905 São Carlos, SP, Brazil*

J.A. Varela

*Instituto de Química, Universidade Estadual Paulista, P.O. Box 355,
14884-970, Araraquara, SP, Brazil*

The effects of heat-treatment temperature on $LiNbO_3$ thin films prepared by the polymeric precursor method were investigated. The precursor solution was deposited on Si(111) substrates by dip coating. X-ray diffraction and thermal analyses revealed that the crystallization process occurred at a low temperature (420 °C) and led to films with no preferential orientation. High-temperature treatments promoted formation of the $LiNb_3O_8$ phase. Scanning electron microscopy, coupled with energy dispersive spectroscopy analyses, showed that the treatment temperature also affected the film microstructure. The surface texture—homogeneous, smooth, and pore-free at low temperature—turned into an "islandlike" microstructure for high-temperature treatments.

I. INTRODUCTION

Lithium niobate ($LiNbO_3$) is an important ferroelectric material because of its excellent piezoelectrical, electro-optical, electroacoustical, pyroelectrical, and photore-fractive properties.[1,2] Because of these physical effects, $LiNbO_3$ presents a large area of applications such as waveguides, optical amplitude and phase modulators, switches, nonvolatile memory elements, surface acoustic wave devices, and second harmonic generators. Using thin films to fabricate the devices is very interesting, especially in the microelectronic industry. The film can be incorporated into current semiconductor technology, which leads not only to the miniaturization device but also to optical loss reduction and a decrease in the final cost. Different methods have been reported for preparing $LiNbO_3$ thin films such as the sol-gel process,[3–6] metalorganic decomposition,[7] pulsed laser deposition,[8,9] liquid-phase epitaxy,[10,11] radiofrequency sputtering,[12,13] and chemical vapor deposition.[14,15]

In this work we prepared $LiNbO_3$ thin films by the polymeric precursor method. This has already been successfully used to prepare lead zirconate titanate (PZT) and $SrTiO_3$ films.[16,17] The global process, outlined in Fig. 1, consists of preparing coating solutions from the Pechini process.[18] Precursor films, deposited by dip coating or spin coating, are then heat treated to eliminate the organic material and to synthesize the phase. The polymeric precursor method presents many advantages, such as the possibility to work in aqueous solutions and a high stoichiometric control. Moreover, it is a low-temperature process and a cost-effective method (inexpensive precursors and little equipment).

This work was carried out to study the effect of heat-treatment temperature on the crystallization and microstructure of $LiNbO_3$ thin films deposited on Si(111) substrates.
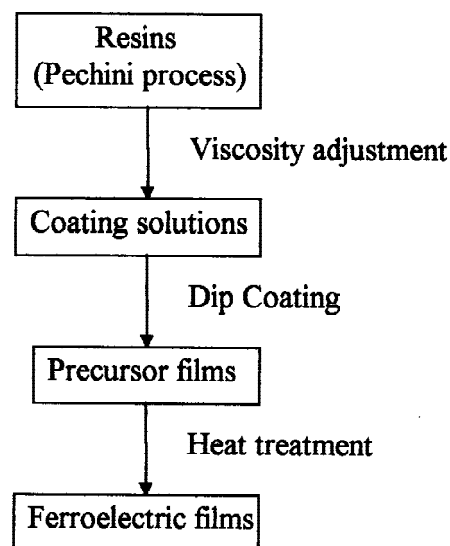

FIG. 1. Flow chart of the thin film preparation process by the polymeric precursor method.

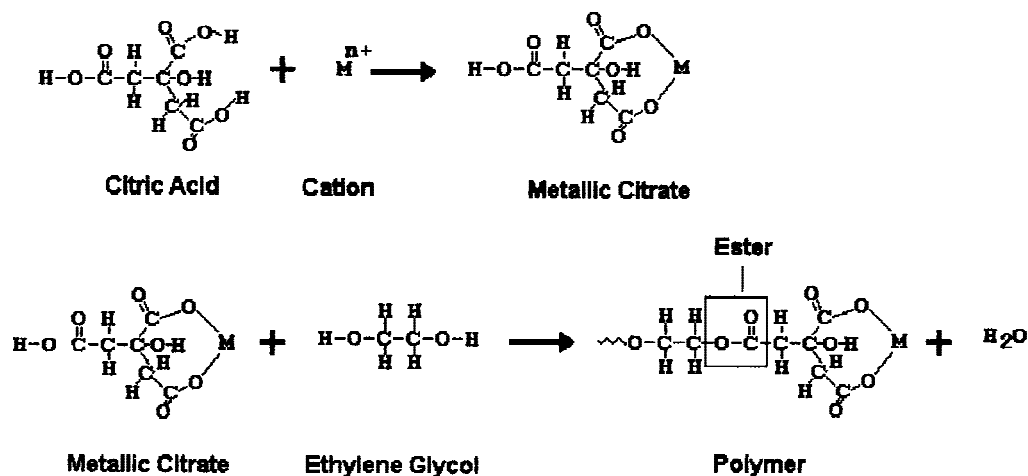[a] Address all correspondence to this author.
e-mail: derl@power.ufsar.br

FIG. 2. Schematic representation of the Pechini process.
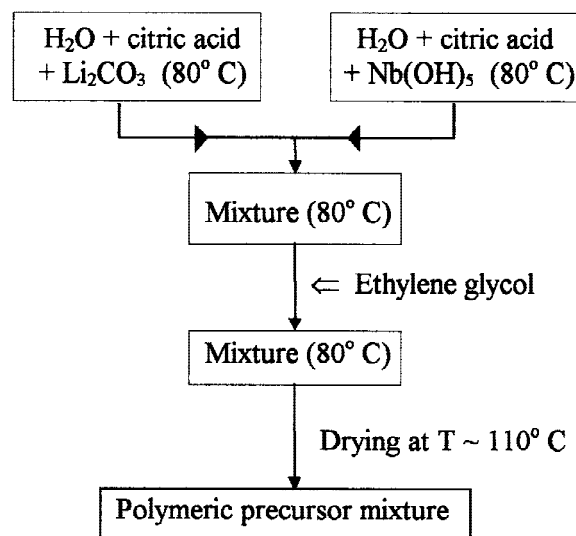
II. EXPERIMENTAL PROCEDURE

A. Coating solution preparation

The polymeric precursor solution was prepared by the Pechini process,[18] which is used to synthesize poly-cations oxides powders.[19–22] This process, outlined in Fig. 2, is based on metallic citrate polymerization with use of ethylene glycol. A hydrocarboxylic acid, such as citric acid, is used to chelate cations in aqueous solution. The addition of a glycol, such as ethylene glycol, leads to organic ester formation. Polymerization, promoted by heating the mixture, results in a homogeneous resin in which metal ions are uniformly distributed throughout the organic matrix.

Figure 3 summarizes preparation of the LiNbO₃ polymeric precursor mixture. A water solution of lithium citrate and a water solution of niobium citrate were prepared separately. The amount of citric acid is determined by the molar ratio citric acid/metal cations and was fixed, in this work, to 3:1. These citric solutions were then mixed (at T ~ 80 °C) and ethylene glycol was added only at the end of the process. The citric acid/ethylene glycol mass ratio was fixed, in this work, to 40:60. The final mixture was dried in an oven (at T ~ 110 °C) to obtain the resin. The viscosity was then adjusted, for the dip-coating process, by adding a controlled amount of water. For this study a coating solution with a viscosity of 10 mPa was used.

B. Thin film preparation

Film deposition was performed by dip coating on (111) silicon substrates. These were cleaned by immersion in a sulfochromic solution followed by rinsing with H₂O and drying in hot air. The precursor films, obtained after one coating (final thickness ~ 40 nm), were heat treated in the range 400–900 °C in ambient air and kept at the annealing temperature for 1 h. The heating and cooling rates used were 1 °C/min.

FIG. 3. Preparation of LiNbO₃ coating solution.

The crystallization process of the prepared films was studied by x-ray diffraction (Siemens, D5000) using grazing incidence and by thermal analyses (DSC, TA Instruments, 2910). The microstructure was observed by scanning electron microscopy (Zeiss, DSM 940A) and chemical analyses by energy dispersive spectroscopy (EDS) were also performed.

III. RESULTS AND DISCUSSION

A. Structural evolution

Figure 4(a) illustrates the x-ray diffraction (XRD) patterns obtained for the films treated at temperatures up to 700 °C. As shown, the film treated at 400 °C is amorphous. At 450 °C peaks related to LiNbO₃ appear, and increasing the temperature results in increased crystallinity. To define with accuracy the temperature that begins the crystallization process, a DSC thermal analysis was
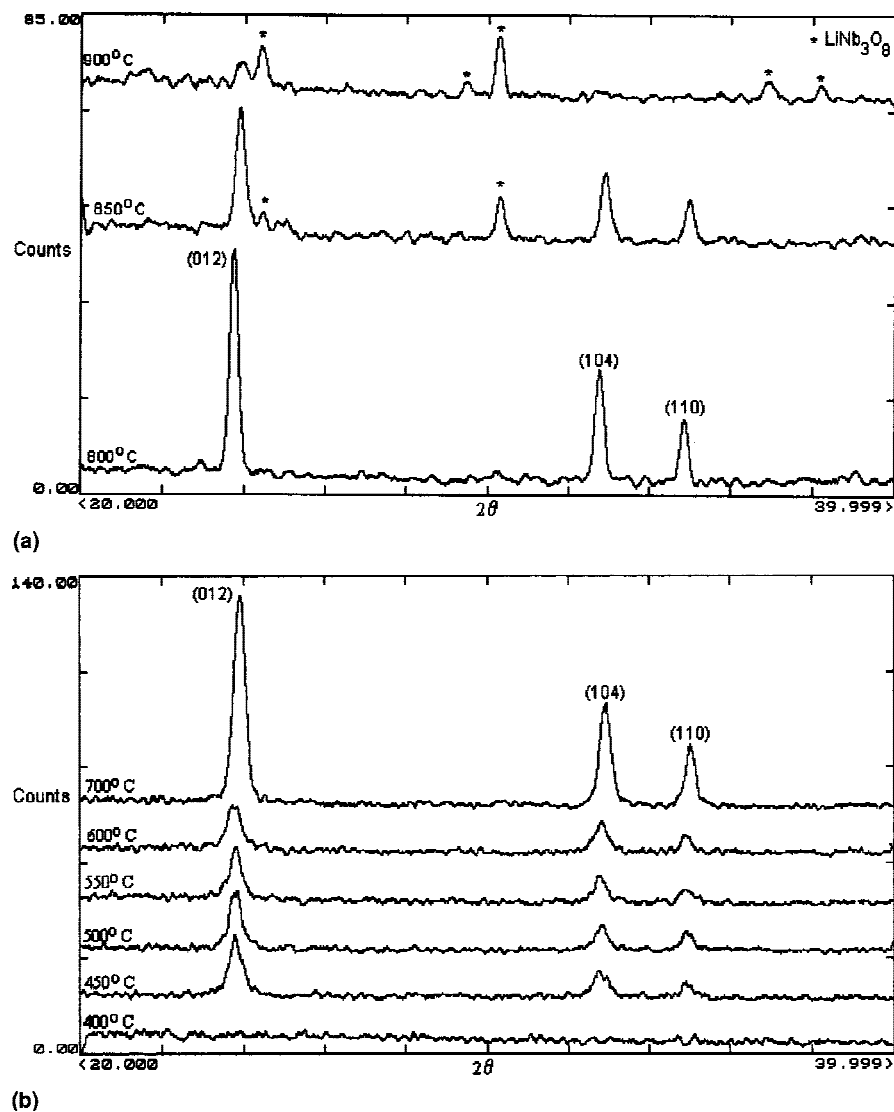
FIG. 4. XRD patterns of films annealed at different temperatures: (a) heat treatment from 400 to 700 °C and (b) heat treatment from 800 to 900 °C.

performed, with a precursor film deposited on Pt substrate, using a heating rate of 1 °C/min. The crystallization peak appears at 420 °C, as shown in Fig. 5. Note that similar crystallization temperatures were reported by several authors[3,4] for LiNbO₃ thin films prepared by sol-gel. Other exothermic peaks are observed below the crystallization peak, which must be related to pyrolysis of the organic precursors.

The XRD patterns show also that the films present no preferential orientation—that is, the films are polycrystalline. This result is not surprising because the silicon presents a crystal structure and lattice parameters different in relation to the LiNbO₃ and therefore makes epitaxial growth difficult. However, Liu *et al.*[23] have already reported oriented LiNbO₃ films deposited on a silicon wafer by pulsed laser deposition. The textured growth was obtained with an electric field during deposition and in situ postannealing.
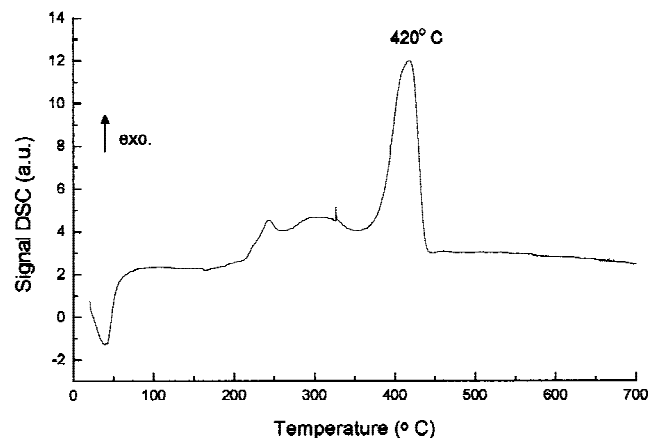

FIG. 5. DSC analysis of a precursor solution deposited on Pt substrate.

Figure 4(b) illustrates the XRD patterns obtained for the films heat treated in the range 800–900 °C. For treatment at 800 °C, the only peaks observed are related to $LiNbO_3$. On the other hand, from 850 °C other peaks appeared that are characteristic of the $LiNb_3O_8$ phase. This result suggests that at high temperature, there is a lithium loss, which leads to $LiNb_3O_8$ formation. This lithium deficiency may be due to its volatile loss during high temperature annealing or it may originate from an interface reaction between the silicon oxidized surface and the lithium niobate to form an amorphous silicate, as proposed in Eq. (1):

$$3LiNbO_3 + SiO_2 \rightarrow LiNb_3O_8 + Li_2SiO_3 \qquad (1)$$

Heat treatments at high temperature (from 800 to 950 °C for 1 h) were performed on the resin and the XRD patterns of the obtained powders revealed only peaks characteristic of $LiNbO_3$. However, it is possible that the $LiNb_3O_8$ phase is also present in the treated powders but is not detected because of its very low concentration. On the other hand, the vapor pressure of Li_2O is relatively low in this temperature range: 6.305×10^{-10} Pa and 4.843×10^{-6} Pa at 727 and 927 °C, respectively.[24] Consequently, the lithium deficiency, leading to the $LiNb_3O_8$ phase formation observed in films treated at high temperature, is probably mainly due to an interface reaction. The volatile loss of Li can contribute to the process but is probably small. Further investigations will be performed, in particular to prove the presence of an eventual amorphous silicate as suggested in Eq. (1).

B. Microstructure study

Figures 6(a)–6(d) show micrographs of the films heat treated up to 600 °C. The films are not only crack-free but also appear relatively dense. However, at 700 °C a more porous microstructure is observed [Fig. 7(a)] and for higher temperatures the films are no more continuous, as shown in Figs. 7(b)–7(d). The microstructure is composed of "islands" whose size increases with temperature. Moreover, whereas the films treated at low temperature are very smooth [Figs. 8(a) and 8(b)], those treated at high temperature are rough [Figs. 8(c) and 8(d)] because of the island formation.

Some authors have already reported such microstructural evolution. Ono *et al.*[5] observed that LiNbO₃ films, prepared on sapphire from an aqueous solution, present a smooth texture without cracks and pores below 500 °C but heat treatment at 600 or 700 °C causes grain growth and deteriorates the film surface. Similar results were also obtained by Braunstein *et al.*[7] with LiNbO₃
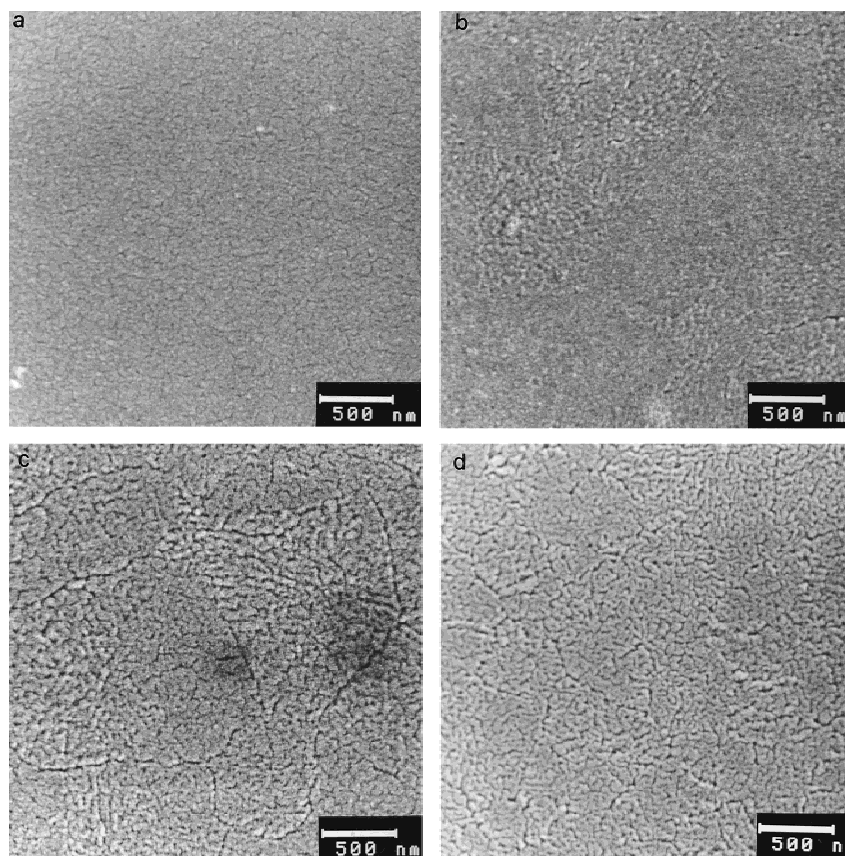

FIG. 6. Micrographs of films treated at different temperatures: (a) 400 °C, (b) 450 °C, (c) 500 °C, and (d) 600 °C.
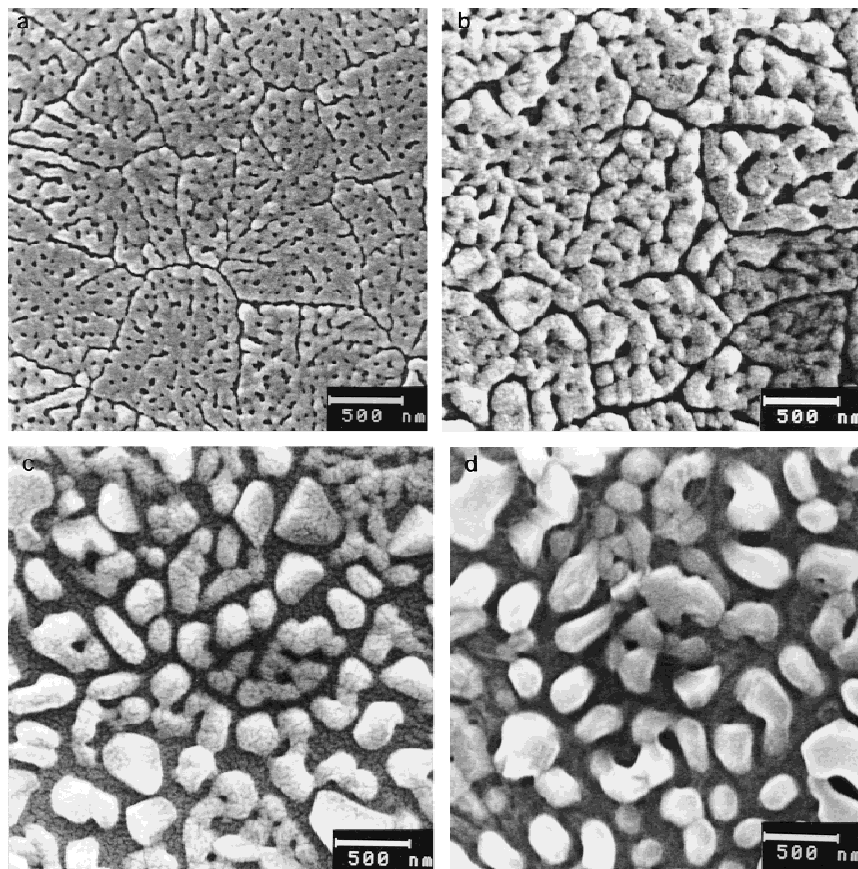
FIG. 7. Micrographs of films treated at different temperatures: (a) 700 °C, (b) 800 °C, (c) 850 °C, and (d) 900 °C.

films prepared on sapphire by metal organic decomposition. According to the authors, the change of the film surface texture with increased heat-treatment temperature would be due to surface tension effects, which become predominant at high temperature and force the formation of a network of discrete droplets.

In this study, island formation started at 700 °C and is probably due to a natural thermodynamic process driven by interface energy—i.e., surface energy of the film and film–substrate interfacial energy. Of course, formation of the interface phase as a result of film–substrate reaction could lead the change in interface energy. The LiNb$_3$O$_8$ phase was observed only from 850 °C but it is possible that its formation started at 700 °C and was not detected from XRD because of its very low concentration at that temperature. In this case, the eventual interface reaction may accelerate or may be the primary force for the island formation process.

C. EDS analyses

Figure 9 shows the EDS analyses performed on the film treated at 550 °C. The x-ray maps [Fig. 9(a)] reveal the distribution of the elements constituting the sample (oxygen, silicon, and niobium) and the region of the film that has been analyzed. Note that this technique does not allow detection of light elements such as lithium. Moreover, the silicon, coming from the substrate, was detected due to electron beam penetration (~1 μm), which is larger than the film thickness (~40 nm). As shown, the film is very homogeneous. This result is confirmed by point analyses performed in two different regions [Fig. 9(b)]: each peak characteristic of an element (Nb, O, Si) has exactly the same intensity and the same area for these two regions.

The EDS results obtained for the film treated at 900 °C are illustrated in Fig. 10. The film islands can be observed on the image of the analyzed region. The x-ray maps show that the element distribution is very inhomogeneous. In particular, it appears that the regions with higher concentrations of niobium correspond to island regions. Spectra have been prepared in two regions [Fig. 10(b)]: the first corresponds to a large island group and the second presents only a few small islands. Note that it is impossible to analyze a region without islands because of the technique resolution. The niobium peak appears more intense in the first region, which indicates that the islands are composed, at 900 °C, of a rich niobium phase like LiNb$_3$O$_8$.

The experimental results suggest that an eventual interface reaction between LiNbO$_3$ and SiO$_2$, formed dur-
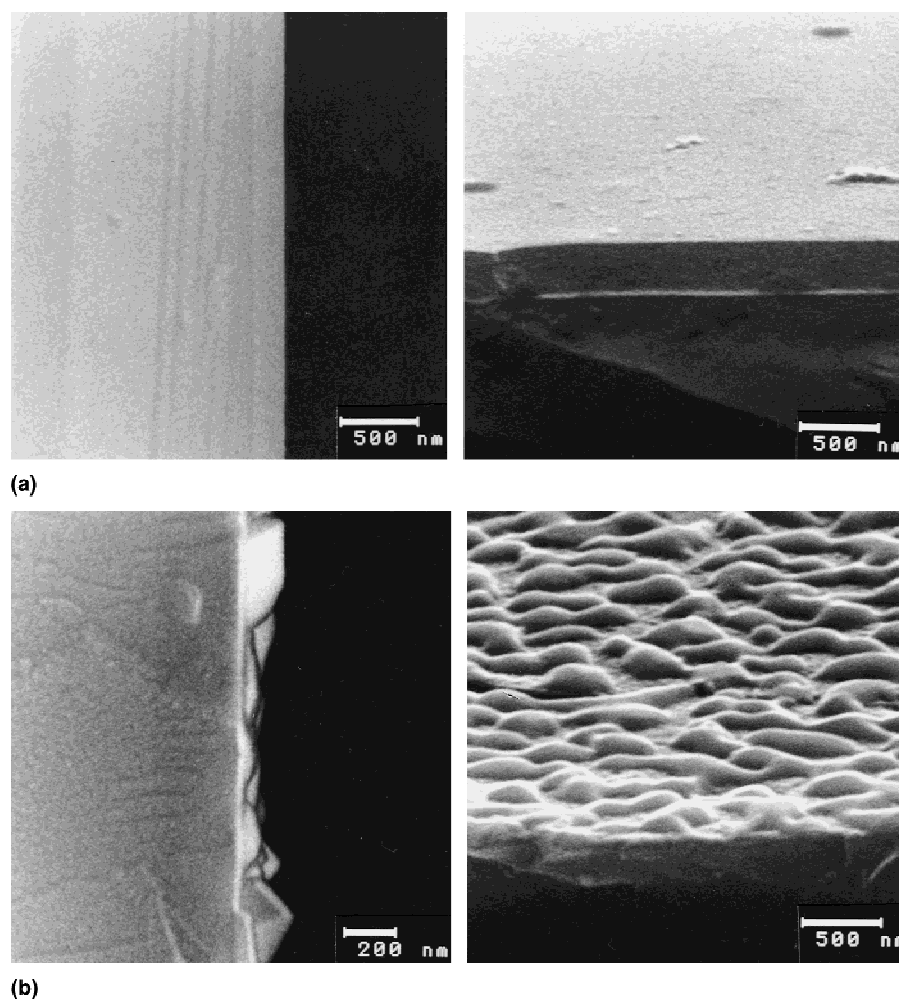
FIG. 8. Micrographs of films obtained at 90° and 75° inclinations: (a) heat treatment at 400 °C and (b) heat treatment at 900 °C.
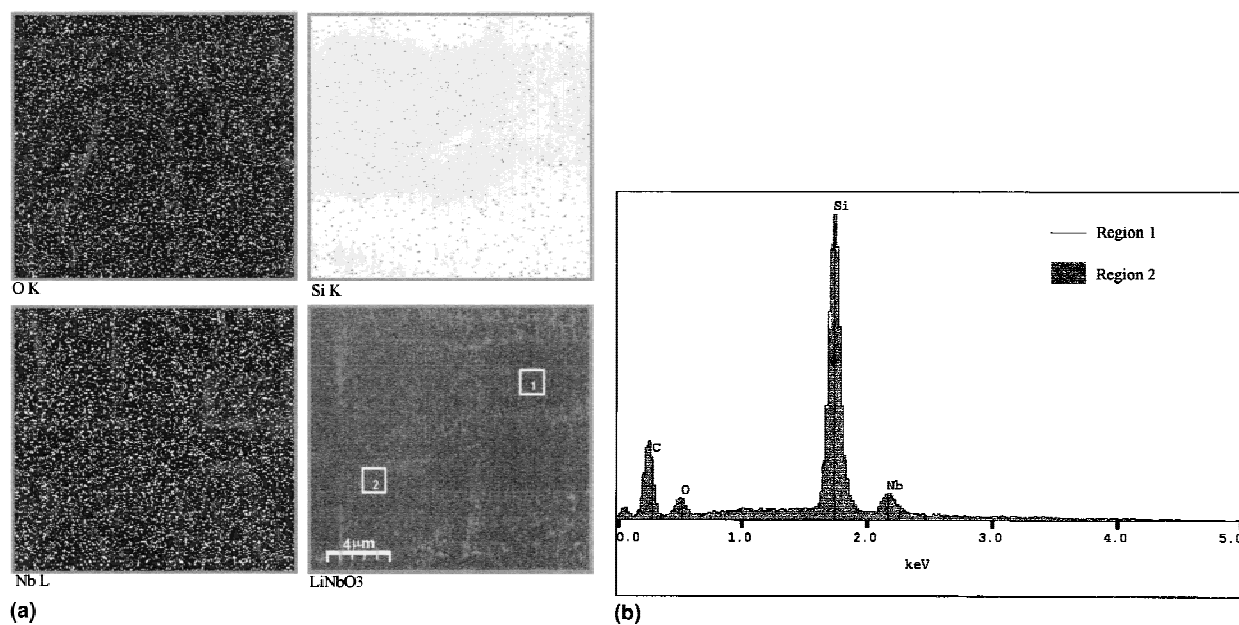

FIG. 9. EDS analyses of film treated at 550 °C: (a) maps of the element distribution and (b) spectra prepared in two different regions.
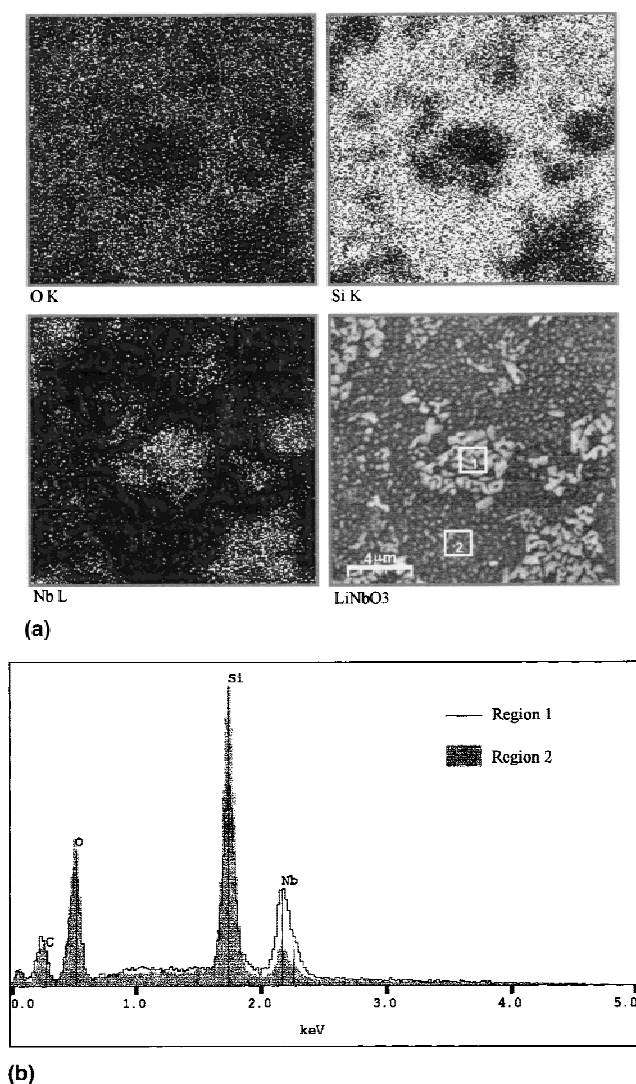
(a)

(b)

FIG. 10. EDS analyses of a film treated at 900 °C: (a) maps of element distribution and (b) spectra prepared in two different regions.

ing the heat treatment at high temperature, leads to formation of lithium silicate (amorphous) and LiNb$_3$O$_8$ (crystalline). This reaction could promote or accelerate the formation of isolated islands. To prevent this interface reaction, a buffer layer or another type of substrate such as sapphire can be used.

IV. CONCLUSION

This work showed that LiNbO$_3$ thin films can be prepared from the polymeric precursor method. The crystallization process occurred at a low temperature (420 °C), which makes this method interesting. The films, deposited on silicon substrates, did not present any preferential orientation and appeared homogeneous (crack-free and dense) and showed smooth surfaces for heat treatments up to 600 °C. For higher heat-treatment

temperatures, formation of LiNb$_3$O$_8$ and an islandlike microstructure resulting in a heterogeneous and rough surface were observed. Formation of the phase poor in lithium may be the result of an interface reaction between the film and the silicon substrate, at high temperature, leading to a stoichiometric deviation.

REFERENCES

1. R.S. Weis and T.K. Gaylord, Appl. Phys. A**37,** 191 (1985).
2. A. Ballman, J. Am. Ceram. Soc. **48,** 112 (1965).
3. K. Terabe, N. Iyi, K. Kitamura, and S. Kimura, J. Mater. Res. **10,** 1779 (1995).
4. K. Nashimoto, M.J. Cima, P.C. Mcintyre, and W.E. Rhine, J. Mater. Res. **10,** 2564 (1995).
5. S. Ono, T. Takeo, and S. Hirano, J. Amer. Ceram. Soc. **79,** 1343 (1996).
6. J.G. Yoon and K. Kim, Appl. Phys. Lett. **68,** 2523 (1996).
7. G. Braunstein, G.R. Paz-Pujalt, and T.N. Blanton, Thin Solid Films **264,** 4 (1995).
8. P. Aubert, G. Garry, R. Bisaro, and J. Garcia Lopez, Appl. Surface Sci. **86,** 144 (1995).
9. S.H. Lee, T.W. Noh, and J.H. Lee, Appl. Phys. Lett. **68,** 472 (1996).
10. A. Yamada, H. Tamada, and M. Saitoh, J. Appl. Phys. **76,** 1776 (1994).
11. T. Kawaguchi, D-H. Yoon, M. Minakata, Y. Okada, M. Imaeda, and T. Fukuda, J. Crystal Growth **152,** 87 (1995).
12. S. Tan, T. Gilbert, C.Y. Hung, T.E. Schlesinger, and M. Migliuolo, J. Appl. Phys. **79,** 3548 (1996).
13. T. Nishida, M. Shimizu, T. Horiuchi, T. Shiosaki, and K. Matsushige, Jpn. J. Appl. Phys. **34**(9B), 5113 (1995).
14. Y. Sakashita and H. Segawa, J. Appl. Phys. **77**(11), 5595 (1995).
15. R.S. Feigelson, J. Crystal Growth **166**(1–4), 1 (1996).
16. V. Bouquet, S.M. Zanetti, C.R. Forschini, E.R. Leite, E. Longo, and J.A. Varela, in *Innovative Processing and Synthesis of Ceramics, Glasses, and Composites,* edited by N.P. Bansal, K.V. Logan, and J.P. Singh, (Ceram. Trans. **85,** Am. Ceram. Soc., Westerville, OH, 1997) p. 333.
17. S.M. Zanetti, E. Longo, J.A. Varela, and E.R. Leite, Mat. Lett. **31,** 173 (1997).
18. M.P. Pechini, U.S. Patent No. 3 330 697 (1967).
19. H.U. Anderson, M.J. Pennell, and J.P. Guha, Adv. Ceramics **21,** 91 (1987).
20. P.A. Lessing, Ceramic Bull. **68,** 1002 (1989).
21. M. Cerqueira, R.S. Nasar, E. Longo, E.R. Leite, and J.A. Varela, Mater. Lett. **22,** 181 (1995).
22. E.R. Leite, C.M.G. Sousa, E. Longo, and J.A. Varela, Ceramics Int. **21,** 143 (1995).
23. Z.G. Liu, W.S. Hu, X.L. Guo, J.M. Liu, and D. Feng, Appl. Surface Sci. **109/110,** 520 (1997).
24. *The Oxide Handbook* edited by G.V. Samsonov, (IFI/Plenum, New York, 1973).